Theoret. Appl. Mech., Vol.37, No.3, pp. 203–227, Belgrade 2010

Thermophoresis effects on non-darcy mhd mixed convective heat and mass transfer past a porous wedge in the presence of suction/ injection

P.Loganathan* **P.Puvi Arasu†**

Abstract

An analysis is presented to investigate the effect of thermophoresis particle deposition and variable viscosity on non-Darcy MHD mixed convective heat and mass transfer of a viscous, incompressible and electrically conducting fluid past a porous wedge in the presence of suction/injection. The wall of the wedge is embedded in a uniform non-Darcian porous medium in order to allow for possible fluid wall suction or injection. The governing partial differential equations of the problem, subjected to their boundary conditions, are solved numerically by applying an efficient solution scheme for local nonsimilarity boundary layer analysis. Numerical calculations are carried out for different values of dimensionless parameter in the problem and an analysis of the results obtained show that the flow field is influenced appreciably by the applied magnetic field. The results are compared with those known from

*Department of Mathematics, Anna University, Chennai, India

†E.S. Engineering College,Thudupathi, Erode, India, e-mail: puviarasup@gmail.com

the literature and excellent agreement between the results is obtained.

Keywords: Non similarity transformation, thermophoresis, non-Darcy flow, Forchheimer number, mixed convection and magnetic effect.

NOMENCLATURE

u, v	velocity components in x and y direction
g	Acceleration due to gravity
k	Thermophoretic coefficient
Pr	Prandtl number
T_w	Temperature of the wall
β	Coefficient of thermal expansion
C	Species concentration of the fluid
C_∞	Species concentration away from the wall
σ	Electric conductivity of the fluid
U	Flow velocity away from the wedge
β^*	Concentration expansion coefficients
K	Permeability of the porous medium
T	Temperature of the fluid
T_∞	Temperature far away from the wall
F	Forchheimer number
C_w	Species concentration away from the wall
ρ	Density of the fluid
α	Thermal diffusivity

1 Introduction

Thermophoresis occurs because of kinetic theory in which high energy molecules in a warmer region of liquid impinge on the molecules with greater momentum than molecules from a cold region. This leads to a migration of particles in the direction opposite the temperature gradient,

from warmer areas to cooler areas. Thermophoresis is of practical importance in a variety of industrial and engineering applications including aerosol collection (thermal precipitators), nuclear reactor safety, corrosion of heat exchangers, and micro contamination control. Thermophoresis has important current applications in the production of optical fibers. A modified chemical vapor deposition process is used to build up layers of glass (GeO_2 and SiO_2) by deposition of particles on the tube wall. Thermophoresis can be used in clean rooms to inhibit the deposition of small particles on electronic chips. As the dimensions of the circuit elements are reduced, the potential failures due to micro contamination by particle deposition increase.

The use of thermophoretic heaters has led to a reduction in chip failures. In the same vein there is the potential application of thermophoresis to remove radioactive aerosols from containment domes in the event of a nuclear reactor accident. Thermophoresis principle is utilized to manufacture graded index silicon dioxide and germanium dioxide optical fiber performs used in the field of communications. In light of these various applications, England and Emery [1] studied the thermal radiation effect of an optically thin gray gas bounded by a stationary vertical plate. Raptis [2] studied radiation effect on the flow of a micro polar fluid past a continuously moving plate. Hossain and Takhar [3] analyzed the effect of radiation using the Rosseland diffusion approximation on mixed convection along a vertical plate with uniform free stream velocity and surface temperature. Duwairi and Damesh [4, 5], Duwairi [6], Damesh et al. [7] studied the effect of radiation and heat transfer in different geometry for various flow conditions.

In certain porous media applications such as those involving heat removal from nuclear fuel debris, underground disposal of radioactive waste material, storage of food stuffs, and exothermic and/or endothermic chemical reactions and dissociating fluids in packed-bed reactors, the working fluid heat generation (source) or absorption (sink) effects are important. In the application of pigments, or chemical coating of metals, or removal of particles from a gas stream by filtration, there can be distinct advantages in exploiting deposition mechanisms to improve efficiency. Goldsmith and May [8] first studied the thermophoretic transport involved in a simple one-dimensional flow for the measurement of the

thermophoretic velocity. thermophoresis in laminar flow over a horizontal flat plate has been studied theoretically by Goren [9]. Thermophoresis in natural convection with variable properties for a laminar flow over a cold vertical flat plate has been studied by Jayaraj et al.[10]. Selim et al.[11] studied the effect of surface mass flux on mixed convective flow past a heated vertical flat permeable plate with thermophoresis. The first analysis of thermophoretic deposition in geometry of engineering interest appears to be that of Hales et al.[12]. They have solved the laminar boundary layer equations for simultaneous aerosol and steam transport to an isothermal vertical surface situated adjacent to a large body of an otherwise quiescent air-steam-aerosol mixture. Simon [13] studied the effect of thermophoresis of aerosol particles in the laminar boundary layer on a flat plate. Recently, Chamkha and Pop [14] studied the effect of thermophoresis particle deposition in free convection boundary layer from a vertical flat plate embedded in a porous medium.

Effects of heat and mass transfer on non-Darcy mixed convection flow in the presence of suction / injection have been studied by many authors in different situations. But so far no attempt has been made to analyze the effects of thermophoresis particle deposition on non-Darcy MHD mixed convective heat and mass transfer past a porous wedge in the presence of suction or injection and hence we have considered the problem of this kind. The order of chemical reaction in this work is taken as first-order reaction. It is hoped that the results obtained will not only provide useful information for applications, but also serve as a complement to the previous studies.

2 Formulation of the problem

Let us consider a steady, laminar, hydromagnetic coupled heat and mass transfer by mixed convection flow in front of a stagnation point on a wedge plate embedded in porous medium. The fluid is assumed to be Newtonian, electrically conducting and its property variations due to temperature are limited to density and viscosity. The density variation and the effects of the buoyancy are taken into account in the momentum equation (Boussinesq's approximation) and the concentration of species far from the wall,

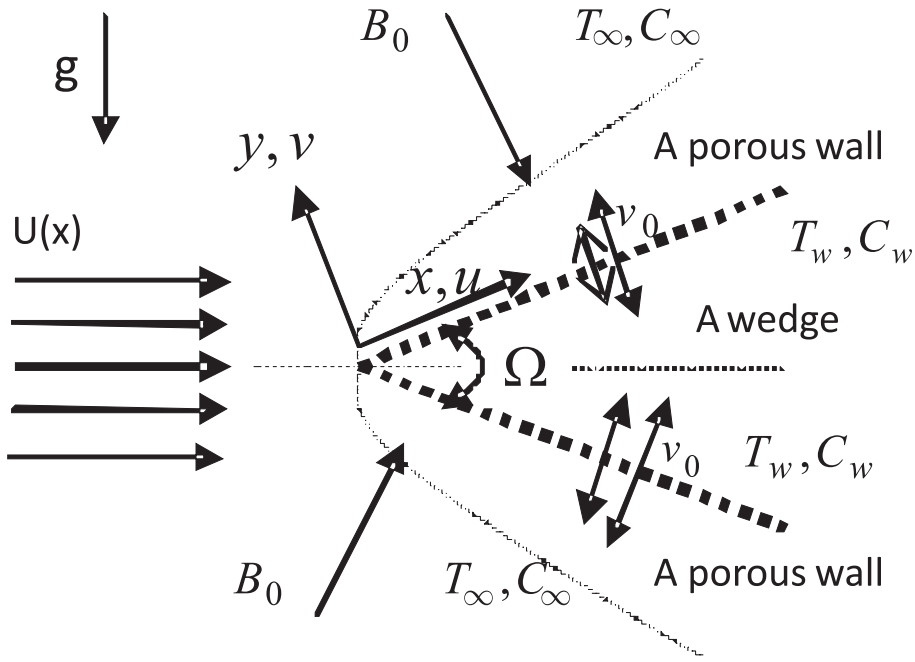

Figure 1: Flow analysis along the wall of the wedge

C_∞, is infinitesimally small. Let the x-axis be taken along the direction of the wedge and y-axis normal to it. A uniform transverse magnetic field of strength B_0 is applied parallel to the y-axis. The chemical reaction is taking place in the flow and the effect of thermophoresis is being taken into account to help in the understanding of the mass deposition variation on the surface. Fluid suction or injection is imposed at the wedge surface, see Fig.1. The viscous dissipation effect and Joule heat are neglected on account of the fluid is finitely conducting. It is assumed that the induced magnetic field, the external electric field and the electric field due to the polarization of charges are negligible. Under these conditions, the governing boundary layer equations of momentum, energy and diffusion for mixed convection flow neglecting Joule's viscous dissipation under Boussinesq's approximation including variable viscosity, Lanndau and Lifshitz [25].

The fundamental equations for steady incompressible flow can be de-

fined as follows:

Conservation of mass:

$$div\ \vec{V}\ = 0 \tag{1}$$

Conservation of linear momentum:

$$(\vec{V}\ .\ grad\ \vec{V})\ = -\frac{1}{\rho}\ grad\ p + \nu\ \nabla^2\ \vec{V} + \vec{F} \tag{2}$$

Conservation of energy:

$$(\vec{V}.\ grad)T = \ \frac{k_e}{\rho\ c_p}\ \nabla^2 T \tag{3}$$

Conservation of diffusion:

$$(\vec{V}.\ grad)C = \ D\ \nabla^2\ C\ -\ (div\ \vec{v}_T C) \tag{4}$$

where $\vec{V}$ the velocity vector, p is the pressure, ν is the kinematic coefficient of viscosity and $\vec{g}$ is the acceleration due to gravity.

Under these conditions, the basic governing boundary layer equation of momentum, energy and diffusion for mixed convection flow neglecting Joule's viscous dissipation under Boussinesq's approximation including variable viscosity, Lanndau and Lifshitz [25] can be simplified to the following equations:

$$\frac{\partial u}{\partial x} + \frac{\partial v}{\partial y} = 0 \tag{5}$$

$$u\frac{\partial u}{\partial x} + v\frac{\partial u}{\partial y} = \frac{1}{\rho}\frac{\partial}{\partial y}(\mu\frac{\partial u}{\partial y}) + U\frac{dU}{dx} - \frac{\sigma B_0^2}{\rho}(u-U) - \frac{\nu}{K}(u-U) - \frac{F}{\sqrt{K}}(u^2-U^2) + (g\beta(T-T_\infty) + g\beta^*(C-C_\infty))\sin\frac{\Omega}{2} \tag{6}$$

$$u\frac{\partial T}{\partial x} + v\frac{\partial T}{\partial y} = \alpha\frac{\partial^2 T}{\partial y^2} \tag{7}$$

$$u\frac{\partial C}{\partial x} + v\frac{\partial C}{\partial y} = D\frac{\partial^2 C}{\partial y^2}\ - \frac{\partial(V_T C)}{\partial y} \tag{8}$$

The boundary conditions are,

$$u = 0,\ v = -v_0,\ T = T_w,\ C = C_w \ at\ y = 0 \tag{9}$$

$$u = U(x),\ T = T_\infty,\ C = C_\infty \ at\ y \to \infty \tag{10}$$

where D is the effective diffusion coefficient; K is the permeability of the porous medium, $V_T(= -k\frac{\nu}{T}\frac{\partial T}{\partial y})$ is the thermophoretic velocity, where k is the thermophoretic coefficient and F is the empirical constant in the second order resistance. As neglecting the convective term, viscous term and setting $F = 0$ in Eq.(2) is reduced to the Darcy law, Bejan [20]. The fourth and fifth terms on the right-hand side of Eq. (2) stand for the first-order (Darcy) resistance and second-order (porous inertia) resistance, respectively. The first step was to predict the pressure and velocity within the porous medium. The approach most commonly used for laminar flows was first described by Darcy, who postulated that the pressure drop within the medium is due to viscous stress and is proportional to the velocity. However Darcy's law is not valid for high-velocity flows and a correction term must be included to take account of inertial effects. This term, is known as the Forchheimer term and is a quadratic function of the velocity.

Following the lines of Kafoussias et al., [5], the following change of variables are introduced

$$\eta = (\sqrt{\frac{(1+m)U}{2\nu\, x}})y, \quad \psi = (\sqrt{\frac{2U\nu\, x}{1+m}})f(x,\eta),$$

$$\theta = \frac{T - T_\infty}{T_w - T_\infty} \quad and \quad \phi = \frac{C - C_\infty}{C_w - C_\infty} \tag{11}$$

Under this consideration, the potential flow velocity can be written as

$$U(x) = Ax^m, \quad \beta_1 = \frac{2m}{1+m} \tag{12}$$

where A is a constant and β_1 is the Hartree pressure gradient parameter that corresponds to $\beta_1 = \frac{\Omega}{\pi}$ or a total angle Ω of the wedge.

The continuity equation (5) is satisfied by the stream function $\psi(x, y)$ defined by

$$u = \frac{\partial \psi}{\partial y} \quad and \quad v = -\frac{\partial \psi}{\partial x} \tag{13}$$

The equations (6) to (8) become

$$\frac{\partial^3 f}{\partial \eta^3} = -f\frac{\partial^2 f}{\partial \eta^2} - \frac{2m}{1+m}(1-(\frac{\partial f}{\partial \eta})^2) - \frac{2}{1+m}\gamma_1(\theta + N\phi)\sin\frac{\Omega}{2}$$

$$+\frac{2x}{1+m}(\frac{\partial f}{\partial \eta}\frac{\partial^2 f}{\partial x \partial \eta} - \frac{\partial f}{\partial x}\frac{\partial^2 f}{\partial \eta^2}) + \frac{2x}{m+1}(\frac{\sigma B_0^2}{\rho U})(\frac{\partial f}{\partial \eta} - 1) + \tag{14}$$

$$\frac{2}{m+1}\lambda(\frac{\partial f}{\partial \eta} - 1) + \frac{2}{m+1}(\frac{Fx}{\sqrt{K}})((\frac{\partial f}{\partial \eta})^2 - 1) + \frac{\partial \theta}{\partial \eta}\frac{\partial^2 f}{\partial \eta^2}$$

$$\frac{\partial^2 \theta}{\partial \eta^2} = -\Pr\frac{\partial \theta}{\partial \eta} + \frac{2\Pr}{1+m}\theta\frac{\partial f}{\partial \eta} + \Pr\frac{2x}{1+m}(\frac{\partial f}{\partial \eta}\frac{\partial \theta}{\partial x} - \frac{\partial f}{\partial x}\frac{\partial \theta}{\partial \eta}) \tag{15}$$

$$\begin{aligned}\frac{\partial^2 \phi}{\partial \eta^2} &= -Sc\,(f - \tau\frac{\partial \theta}{\partial \eta})\frac{\partial \phi}{\partial \eta} + \frac{2\,Sc}{1+m}\phi\frac{\partial f}{\partial \eta} + \\ &\quad \frac{2xSc}{1+m}(\frac{\partial f}{\partial \eta}\frac{\partial \phi}{\partial x} - \frac{\partial f}{\partial x}\frac{\partial \phi}{\partial \eta}) + Sc\tau\frac{\partial^2 \theta}{\partial \eta^2}\phi\end{aligned} \tag{16}$$

where the Grashof number Gr_x, Local buoyancy parameter γ_1, Sustentation parameter N, Reynolds number Re_x, Modified local Reynolds number Re_k, Prandtl number Pr, Forchheimer number F_n, Schmidt number Scs magnetic parameter M^2, suction/injection parameter S, thermophoresis particle deposition parameter τ and porous medium parameter λ, are defined as

$$Gr_x = \frac{g\beta x^3(T_w - T_\infty)}{\nu^2},\ \gamma_1 = \frac{Grx}{Rex^2},\ Re_x = \frac{Ux}{\nu},\ Re_k = \frac{U\sqrt{K}}{\nu},\ \Pr = \frac{\nu}{\alpha}$$

(where α is the effective thermal diffusivity of the porous medium),

$$F_n = \frac{FU\sqrt{K}}{\nu},\ Sc = \frac{\nu}{D},\ M^2 = \frac{\sigma B_0^2}{\rho\, A},$$

$$S = v_0\sqrt{\frac{(1+m)x}{2\,\nu\,U}},\quad \tau = -\frac{k(T_w - T_\infty)}{T_r}\quad and\quad \lambda = \frac{\alpha}{K\ A} \tag{17}$$

The boundary conditions can be written as

$$\eta = 0: \quad \frac{\partial f}{\partial \eta} = 0, \quad \frac{f}{2}(1 + \frac{x}{U}\frac{dU}{dx}) + x\frac{\partial f}{\partial x} = -v_0\sqrt{\frac{(1+m)x}{2\nu U}}$$

$$\theta = 1, \ \phi = 1$$

$$\eta \to \infty: \quad \frac{\partial f}{\partial \eta} = 1, \ \theta = 0, \ \phi = 0 \tag{18}$$

where v_0 is the velocity of suction if $v_0 < 0$. F_n is the dimensionless inertial parameter (Forchheimer number) and $\xi = k\, x^{\frac{1-m}{2}}$ Kafoussias and Nanousis [5], is the dimensionless distance along the wedge ($\xi > 0$).

The equations (14) to (16) and boundary conditions (18) can be written as

$$\frac{\partial^3 f}{\partial \eta^3} + f\frac{\partial^2 f}{\partial \eta^2} - \frac{2}{1+m}M^2\xi^2(\frac{\partial f}{\partial \eta} - 1) + \frac{2}{1+m}\gamma_1(\theta + N\phi)\sin\frac{\Omega}{2} -$$

$$\frac{2}{m+1}\xi^2\lambda\,\mathrm{Pr}(\frac{\partial f}{\partial \eta} - 1\ ) - \frac{2}{m+1}((\frac{\partial f}{\partial \eta})^2 - 1\ )(\frac{Rex}{Re_k^2}F_n + m) -$$

$$\frac{2}{1+m}\frac{\partial \theta}{\partial \eta}\,\frac{\partial^2 f}{\partial \eta^2} = -\frac{1-m}{1+m}\left[f''\left(\xi\frac{\partial f}{\partial \xi}\right) - f'\left(\xi\frac{\partial f'}{\partial \xi}\right)\right] \tag{19}$$

$$\frac{\partial^2 \theta}{\partial \eta^2} + \mathrm{Pr}\, f\frac{\partial \theta}{\partial \eta} - \frac{2\,\mathrm{Pr}}{1+m}\theta\frac{\partial f}{\partial \eta} = -\ \mathrm{Pr}\,\frac{1-m}{1+m}\left[\theta'\ \left(\xi\frac{\partial f}{\partial \xi}\right) - f'\left(\xi\frac{\partial \theta}{\partial \xi}\right)\right] \tag{20}$$

$$\frac{\partial^2 \phi}{\partial \eta^2} + Sc\,(f - \tau\frac{\partial \theta}{\partial \eta})\,\frac{\partial \phi}{\partial \eta}\ - \frac{2Sc}{1+m}\phi\frac{\partial f}{\partial \eta}\ - Sc\tau\frac{\partial^2 \theta}{\partial \eta^2}\phi =$$

$$-Sc\frac{1-m}{1+m}\left[\phi'\ \left(\xi\frac{\partial f}{\partial \xi}\right) - f'\left(\xi\frac{\partial \phi}{\partial \xi}\right)\right] \tag{21}$$

$$\eta \quad = \quad 0: \quad \frac{\partial f(\xi,\eta)}{\partial \eta} = 0, \ \frac{(1+m)}{2}f(\xi,\eta) + \frac{1-m}{2}\xi\frac{\partial f(\xi,\eta)}{\partial \xi} = -S,$$

$$\theta(\xi,\eta)=1, \phi(\xi,\eta)=1$$

$$\eta\to\infty: \quad \frac{\partial f(\xi,\eta)}{\partial\eta}=1,\ \theta(\xi,\eta)=0,\ \phi(\xi,\eta)=0 \tag{22}$$

where the prime denotes partial differentiation with respect to η, and the boundary conditions (22) remain the same. This form of the system is the most suitable for the application of the numerical scheme described below.

It may be observed that Equations (19) – (21) remain partial differential equations after transformation, with $\frac{\partial}{\partial\xi}$ terms on the right-hand side. In this system of equations, it is obvious that the nonsimilarity aspects of the problem are embodied in the terms containing partial derivatives with respect to ξ. This problem does not admit similarity solutions. Thus, with ξ-derivative terms retained in the system of equations, it is necessary to employ a numerical scheme suitable for partial differential equations for the solution. Formulation of the system of equations for the local nonsimilarity model with reference to the present problem will now be discussed.

At the first level of truncation, the terms accompanied by $\xi\frac{\partial}{\partial\xi}$ are small. This is particularly true when ($\xi << 1$). Thus the terms with $\xi\frac{\partial}{\partial\xi}$ on the right-hand sides of equations (19) – (21) are deleted to get the following systems of equations:

$$f'''+ff''-\frac{2}{1+m}M^2\xi^2(f'-1)+\frac{2}{1+m}\gamma_1(\theta+N\phi)\sin\frac{\Omega}{2}$$

$$-\frac{2}{m+1}\xi^2\lambda\,\mathrm{Pr}(f'-1)-\frac{2}{m+1}(f\prime^2-1)(\frac{Rex}{Re_k^2}F_n+m)-\frac{2}{1+m}\theta' ff''=0 \tag{23}$$

$$\theta''+\mathrm{Pr}\,f\theta'-\frac{2\,\mathrm{Pr}}{1+m}f'\theta=0 \tag{24}$$

$$\phi''+Sc(f-\tau\theta')\,\phi'-\frac{2Sc}{1+m}\phi\ f'-Sc\tau\theta''\,\phi=0 \tag{25}$$

where $f' = \frac{\partial f}{\partial \eta}, f'' = \frac{\partial^2 f}{\partial \eta^2}$ *and* $f''' = \frac{\partial^3 f}{\partial \eta^3}$ with boundary conditions

$$f'(\xi,0) = 0, \quad \frac{(1+m)}{2} f(\xi,0) + \frac{1-m}{2}\xi \frac{\partial f(\xi,0)}{\partial \xi} = -S,$$

$$\theta(\xi,0) = 1, \quad \phi(\xi,0) = 1$$

$$f'(\xi,\infty) = 1, \quad \theta(\xi,\infty) = 0, \quad \phi(\xi,\infty) = 0 \tag{26}$$

Equations (23) to (25) can be regarded as a system of ordinary differential equations for the functions f, θ *and* ϕ with ξ as a parameter for given pertinent parameters.

The major physical quantities of interest are the local skin friction coefficient; the local Nusselt number and the local Sherwood number are defined, respectively, by:

$$C_f = \frac{f''(\xi,0)}{Re_x^{\frac{1}{2}}}; \; N_u = -\frac{\theta'(\xi,0)}{Re_x^{\frac{1}{2}}} \; \textit{and} \; S_h = -\frac{\phi'(\xi,0)}{Re_x^{\frac{1}{2}}} \tag{27}$$

This form of the system is the most suitable for the application of the numerical scheme described below.

3 Numerical solution

The MHD boundary layer over the wedge, subjected to a velocity of suction or injection, is described by the system of partial differential equations (19) - (21), and its boundary conditions (22). In this system of equations $f(\xi,\eta)$ is the dimensionless stream function; $\theta(\xi,\eta)$ be the dimensionless temperature; $\phi(\xi,\eta)$ be the dimensionless concentration; Pr, the Prandtl number; Re_x, Reynolds number etc. which are defined in (17). It is obvious that the nonsimilarity aspects of the problem are embodied in the terms containing partial derivatives with respect to ξ. Thus, with ξ derivative terms retained in the system of equations (23) - (25), it is necessary to employ a numerical scheme suitable for partial differential equations for the solution. In addition, owing to the coupling between adjacent streamwise locations through the ξ derivatives, a locally autonomous solution, at any given streamwise location, cannot be

obtained. In such a case, an implicit marching numerical solution scheme is usually applied preceding the solution in the ξ-direction, i.e., calculating unknown profiles at $\xi_{\iota+1}$ when the same profiles at ξ_ι are known. The process starts at $\xi = 0$ and the solution proceeds from xi_ι to $\xi_{\iota+1}$ but such a procedure is time consuming.

However, when the terms involving $\frac{\partial f}{\partial \xi}$, $\frac{\partial \theta}{\partial \xi}$ and $\frac{\partial \phi}{\partial \xi}$ and their η derivatives are deleted, the resulting system of equations resembles, in effect, a system of ordinary differential equations for the functions f, θ and ϕ with ξ as a parameter and the computational task is simplified. Furthermore a locally autonomous solution for any given ξ can be obtained because the stream wise coupling is severed.

So, in this work, a modified and improved numerical solution scheme for local nonsimilarity boundary layer analysis is used. The scheme is similar to that of Minkowycz et al. [2], but it deals with the differential equations in lieu of integral equations. In each level of truncation, the governing coupled and nonlinear system of differential equations is solved by applying the common finite difference method, with central differencing, a tridiagonal matrix manipulation, and an iterative procedure. The whole numerical scheme can be programmed and applied easily and has distinct advantages compared to that in Minkowycz et al. [22] with respect to stability, accuracy, and convergence speed. The details of this scheme are described in Kafoussias and Karabis [23] and Kafoussias and Williams [24].

To examine the behavior of the MHD boundary layer over the wedge, numerical calculations were carried out for different values of the dimensionless parameters. The numerical results are shown in Figures 2–8 for the velocity, temperature, and concentration of the fluid along the wall of the wedge.

4 Results and discussion

Numerical computations are carried out for

$$0 \leq \tau,\ M^2 \leq 5;\ 0.01 \leq F_n \leq 0.2; 0.1 \leq \lambda \leq 3.0;$$

$$-3.0 \leq \gamma_1 \leq 1.0;\ -1.5 \leq S \leq 3.0.$$

Typical velocity, temperature and concentration profiles are shown in following Figures for $Pr = 0.71$ and some values for the parameters γ, M^2, τ, γ_1, Sc, m, N and λ. The case $\gamma_1 >> 1.0$ corresponds to pure free convection, $\gamma_1 = 1.0$ corresponds to mixed convection and $\gamma_1 << 1.0$ corresponds to pure forced convection. Throughout this calculation we have considered $\gamma_1 = 1.0$ unless otherwise specified. The velocity, temperature and concentration profiles obtained in the dimensionless form are presented in the following Figures for $Pr = 0.71$ which represents air at temperature 20^0C and $Sc = 0.62$ which corresponds to water vapor that represents a diffusion chemical species of most common interest in air. Grashof number for heat transfer is chosen to be $Gr_x = 9$, since these values corresponds to a cooling problem, and Reynolds number $Re_x = 3.0$.

The computations have been carried out for various values of magnetic parameter (M^2), Forchheimer number (F_n), Thermophoresis particle deposition parameter (τ) and porous medium (λ). In the absence of diffusion equation, in order to validate our method, we have compared steady state results of skin friction $f''(\xi, 0)$ and rate of heat transfer $-\theta'(\xi, 0)$ for various values of ξ (Table.1) with those of Minkowycz et al. [22] and found them in excellent agreement.

	Minkowycz et al.[22]		Present works	
ξ	$f''(\xi, 0)$	$-\theta'(\xi, 0)$	$f''(\xi, 0)$	$-\theta'(\xi, 0)$
0	0.33206	0.29268	0.33206	0.29268
0.2	0.55713	0.33213	0.55707	0.33225
0.4	0.75041	0.35879	0.75007	0.35910
0.6	0.92525	0.37937	0.92449	0.37986
0.8	1.08792	0.39640	1.08700	0.39685
1.0	1.24170	0.41106	1.24062	0.41149
2.0	1.92815	0.46524	1.92689	0.46551
10.0	5.93727	0.64956	5.93502	0.64968

Table 1: Comparison with previous Literature

The velocity and temperature profiles are shown in Fig. 2. It is observed that the absence of diffusion equations, in order to ascertain the accuracy

of our numerical results, the present study is compared with the available exact solution in the literature. The velocity profiles for ξ are compared with the available exact solution of Minkowycz et al. [22], is shown in Fig.2. It is observed that the agreements with the theoretical solution of velocity and temperature profiles are excellent.

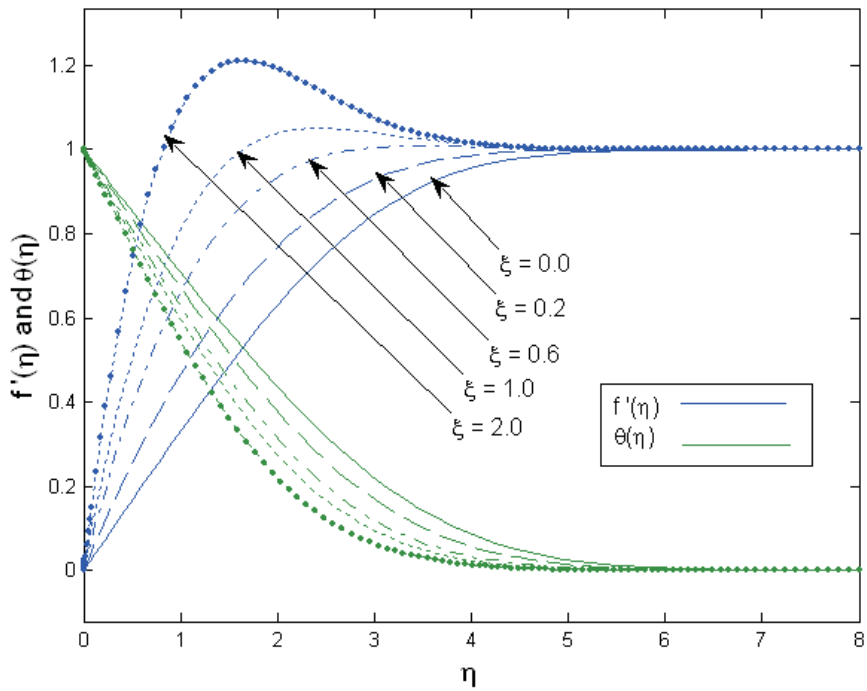

Figure 2: Comparison of the effect of ξ on velocity and temperature profiles

The effects of thermophoretic parameter τ on velocity, temperature and concentration field are shown in Fig.3. It is observed that the velocity, temperature and concentration of the fluid decrease with increase of thermophoretic parameter. In particular, the effect of increasing the thermophoretic parameter τ is limited to increasing slightly the wall slope of the concentration profiles but decreasing the concentration. This is true only for small values of Schmidt number for which the Brownian diffusion effect is large compared to the convection effect. However, for large values

of Schmidt number ($Sc > 100$) the diffusion effect is minimal compared to the convection effect and, therefore, the thermophoretic parameter τ is expected to alter the concentration boundary layer significantly. This is consistent with the work of Goren [12] on thermophoresis of aerosol particles in flat plate boundary layer.

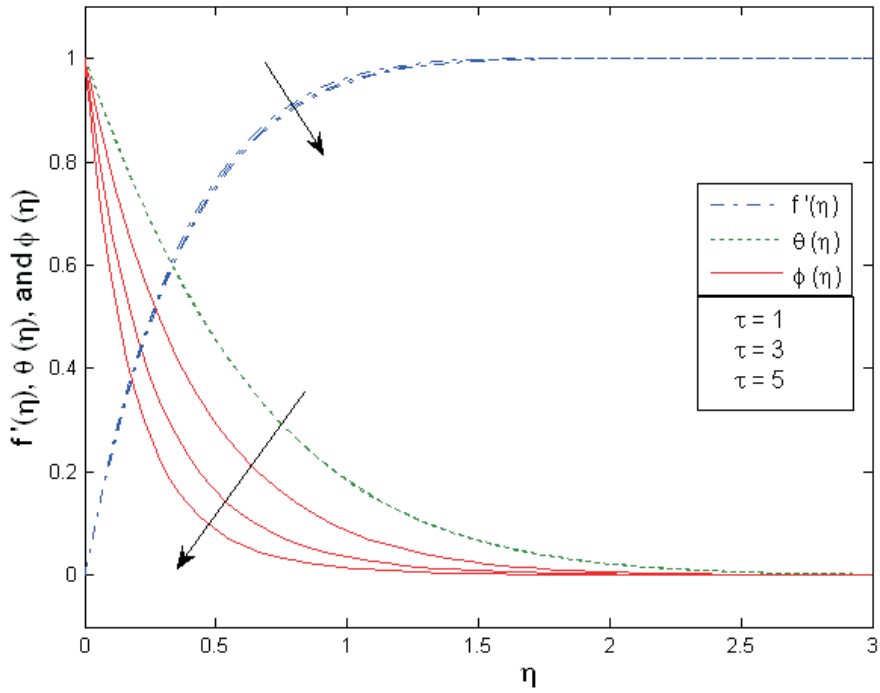

Figure 3: Thermophoretic effect on velocity, temperature and concentration profiles $\gamma_1 = 1.0$, $m = 0.0909$, $N = 3$, $Re_k = M^2 = 1.0$, F_n, $\lambda = 0.1$, $S = 3.0$, $\xi = 0.01$ and $\Omega = 30^0$

Figure 4 presents typical profiles for velocity, temperature and concentration for different values of magnetic parameter. Due to the uniform suction effects, it is clearly shown that the velocity of the fluid increases and the temperature and concentration of the fluid slightly decrease with increase of the strength of magnetic field. The effects of a transverse magnetic field to an electrically conducting fluid gives rise to a resistive-type force called the Lorentz force. This force has the tendency to slow

down the motion of the fluid and to reduce its temperature and concentration profiles. This result qualitatively agrees with the expectations, since magnetic field exerts retarding force on the mixed convection flow. Application of a magnetic field moving with the free stream has the tendency to induce a motive force which decreases the motion of the fluid and increases its boundary layer. This is accompanied by a decrease in the fluid temperature and concentration.

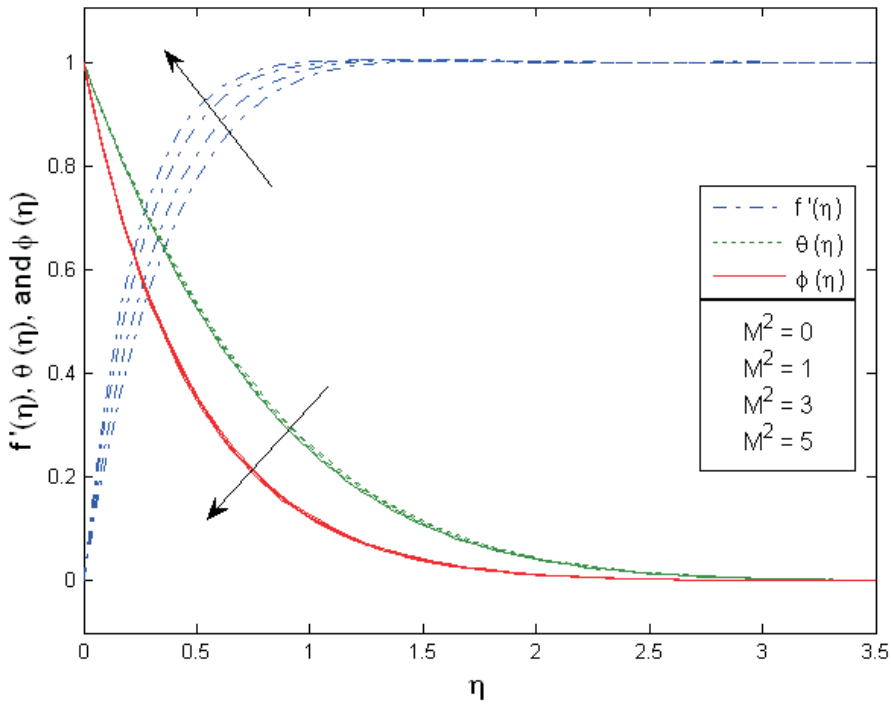

Figure 4: Magnetic effect on velocity, temperature and concentration profiles $\gamma_1 = 1.0$, $m = 0.0909, N = 3$, $Re_k = 1.0$, $F_n = \lambda = 0.1$, $\tau = 0.5$, $S = 3.0$, $\xi = 0.01$ and $\Omega = 30^0$

Figure 5 shows the influence of the inertial parameter F_n on the dimensionless velocity, temperature and concentration profiles, respectively. It is observed that, the velocity increases as the inertial parameter (Forchheimer number) increases. The reason for this behavior is that the inertia of the porous medium provides an additional resistance to the fluid flow

mechanism, which causes the fluid to move at a retarded rate with reduced temperature and concentration. These behaviors are shown in Fig.5. The decreasing of thickness of the concentration layer is caused by the direct action of suction at the wall of the surface. All these physical behavior are the combined effect of thermophoresis particle deposition with suction at the wall of the surface.

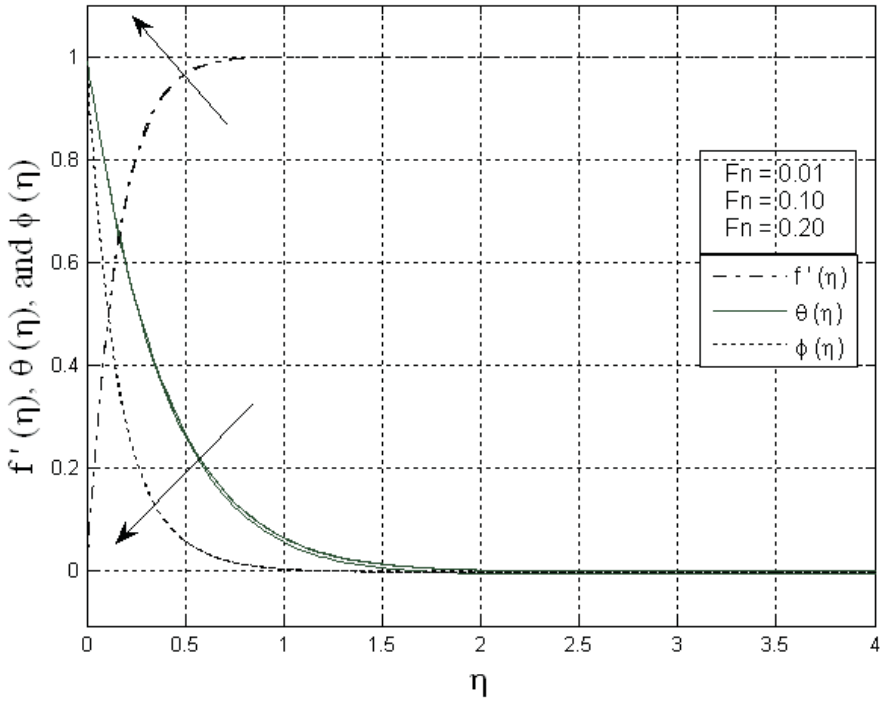

Figure 5: Forchheimer number on velocity, temperature and concentration profiles $\gamma_1 = 1.0$, $m = 0.0909$, $Re_k = M^2 = 1.0$, $\lambda = n = 0.1$, $\tau = 0.5$, $S = 3.0, N = 3.0$, $\xi = 0.01$ and $\Omega = 30^0$

Figure 6 shows the effect of the porosity parameter on the dimensionless velocity, temperature and concentration profiles, respectively. It is observed that the velocity increases as the porosity increases. The reason for this behavior is that the suction of the wall of the wedge provides an additional effect to the fluid flow mechanism, which causes the fluid to

move at a retarded rate with reduced temperature. These behaviors are shown in Fig.6. Also, it is observed that the concentration of the fluid is almost not affected with increase of the porosity parameter.

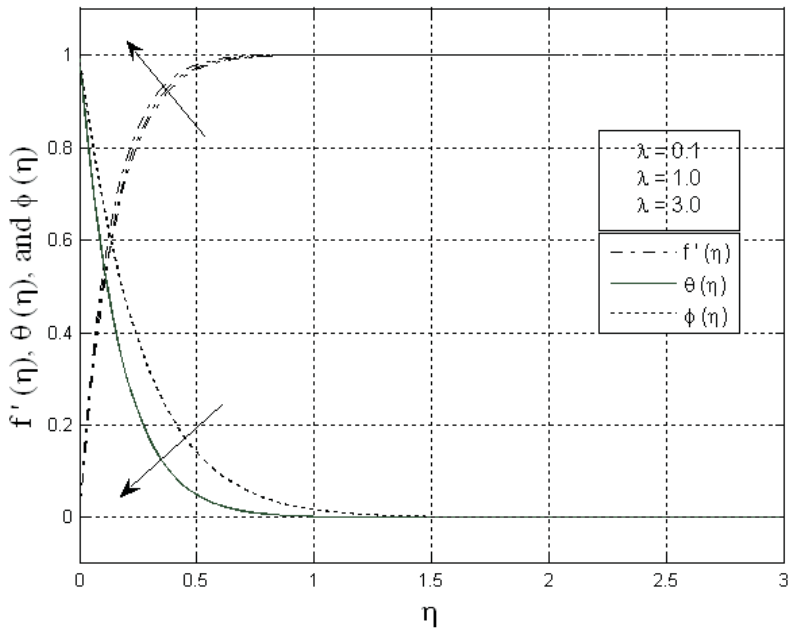

Figure 6: Porosity effects on velocity, temperature and concentration profiles γ_1 = 1.0,m = 0.0909, Re_k= M ^{2}= 1.0, S = 3.0, τ = 0.5, N =3.0,ξ=0.01 and $\Omega = 30^0$

Figure 7 depicts the dimensionless velocity, temperature and concentration profiles for different values of buoyancy parameter. In the presence of uniform magnetic effect, it is seen that the velocity for free convection is more dominant to compare with the forced and mixed convection flow and there is no significant effects on temperature and concentration boundary layer.

Figure 8 illustrates the influence of the suction / injection parameter S on the velocity, temperature and concentration profiles, respectively. The imposition of wall fluid suction for this problem has the effect of

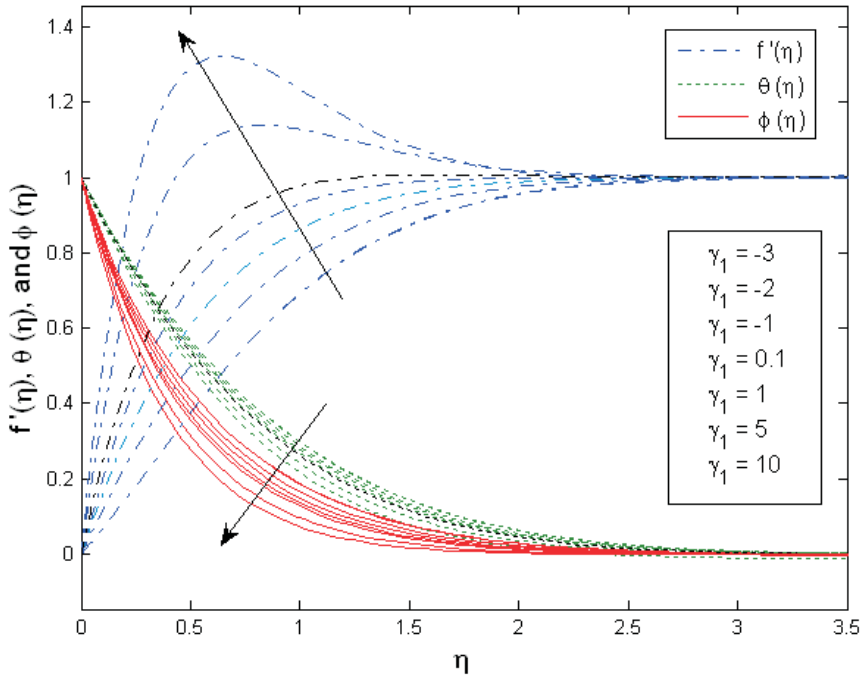

Figure 7: Buoyancy effects on velocity, temperature and concentration profiles γ_1 = 1.0,m = 0.0909, Re_k= M ^{2}= 1.0, S = 3.0, τ = 0.5, N =3.0,ξ= 0.01 and $\Omega = 30^0$

increasing the entire hydrodynamic and reduces the thermal and concentration boundary layers causing the fluid velocity to increase while decreasing its temperature and concentration for suction / injection. It is interesting to note that the velocity of the fluid decreases with increase of injection ($S < 0$). The decreasing of thickness of the concentration layer is caused by two effects; (i) the direct action of suction, and (ii) the indirect action of suction causing a thicker thermal boundary layer, which corresponds to lower temperature gradient, a consequent increase in the thermophoretic force and higher concentration gradient. From the Table 2, it is observed that the skin friction increases and the rate of heat and mass transfer decrease with increase of magnetic and suction parameters respectively, whereas the skin friction and the rate of mass

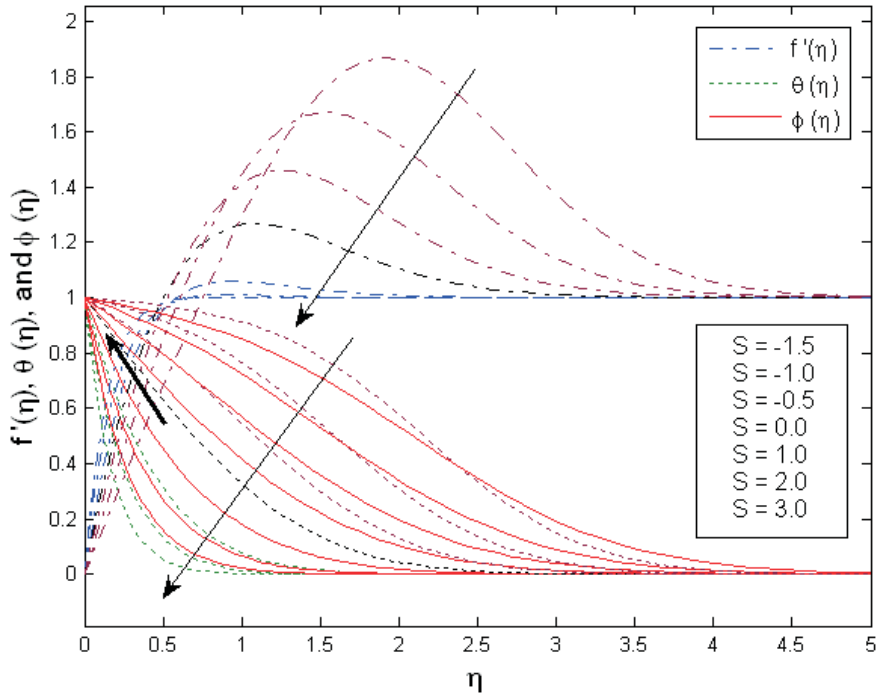

Figure 8: Suction/injection effects on velocity, temperature and concentration profiles $\gamma_1 = 1.0$,m = 0.0909, Re_k= M ^{2}= 1.0, $\tau = 0.5$, N =3.0,ξ= 0.01 and $\Omega = 30^0$

transfer decrease and the rate of heat transfer increases with increase of thermophoretic parameter. It is interesting to note that the skin friction and the rate of mass transfer of forced convection flow is more significant to compare with free and mixed convection whereas the rate of heat transfer of free convection flow is faster to compare with the other two convection flows.

5 Conclusions

In the present paper, the effect of thermophoresis particle deposition on non-Darcy MHD mixed convection boundary layer flow over a porous

$f''(0)$	$\theta'(0)$	$\phi'(0)$		Parameter
6.034338	-2.580389	-5.260410	$\tau = 1.0$	Thermophoretic
6.034184	-2.580390	-6.804620	$\tau = 2.0$	
6.034067	-2.580391	-8.366696	$\tau = 3.0$	
6.176755	-5.772941	-3.716062	$M^2 = 0.1$	Magnetic
7.335917	-5.791495	-3.732215	$M^2 = 5.0$	
8.267194	-5.804222	-3.744466	$M^2 = 10.0$	
7.899134	-7.543495	-4.788675	S = 4.0	Suction
9.665340	-9.336595	-5.882326	S = 5.0	
11.459151	-11.141771	-6.988321	S = 6.0	
7.284197	-5.789842	-3.757063	$\gamma_1 = 0.1$	Forced convection
7.357326	-5.791082	-3.758139	$\gamma_1 = 1.0$	Mixed convection
7.681770	-5.796572	-3.762913	$\gamma_1 = 5.0$	Free convection

Table 2: Analysis for skin friction and rate of heat and mass transfer

wedge in the presence of suction or injection has been studied numerically. There are many parameters involved in the final form of the mathematical model. The problem can be extended on many directions, but the first one seems to be to consider the effects of thermophoresis particle deposition. In mixed convection regime, the concentration boundary layer thickness decreases with increase of the thermophoretic parameter. So, the thermophoretic effects in the presence of magnetic field have a substantial effect on the flow field and, thus, on the heat and mass transfer rate from the sheet to the fluid. As the suction and inertial parameter increase, the hydrodynamic boundary layer increases and the thermal and concentration boundary layers decrease. Thermophoresis is an important mechanism of micro-particle transport due to a temperature gradient in the surrounding medium and has found numerous applications, especially in the field of aerosol technology. It is expected that this research may prove to be useful for the study of movement of oil or gas and water through the reservoir of an oil or gas field, in the migration of under ground water and in the filtration and water purification processes.

References

[1] Gehart,B., and Pera,L.,1971, The nature of vertical natural convection flows resulting from the combined buoyancy effects of thermal and mass diffusion, Int. J. Heat Mass Transfer, **14,** 2025.

[2] Byron Bird, R., Stewart, W.E., Lightfoot, E. N., 1992, Transport Phenomena, John Wiley & sons, New York.

[3] Cussler, E.L., 1988, Diffusion Mass Transfer in Fluid Systems, Cambridge University Press, London, UK.

[4] Yih, K.A., 1998, Uniform suction / blowing effect on force convection about wedge, Acta Mechanica, **128**, 173.

[5] Kafoussias, N.G.; Nanousis, N.D., 1997, Magnetohydrodynamic laminar boundary layer flow over a wedge with suction or injection. Can, J. Physics., **75**, 733.

[6] Watanabe, T., 1990, Thermal boundary layer over a wedge with uniform suction or injection in forced flow, Acta Mechanica, **83**, 119.

[7] Apelblat, A., 1982, Mass transfer with a chemical reaction of the first order, Che. Engg. J. **23**, 193.

[8] Das, U.N., Deka, R and Soundalgekar, 1994, Effects of mass transfer on flow past an impulsively started infinite vertical plate with constant heat flux and chemical reaction, Forschung im Ingenieurwesen, **60**, 284.

[9] Muthucumaraswamy, R and Ganesan, P., 2001, Effects of the chemical reaction and injection on flow characteristics in an unsteady upward motion of an isothermal plate, J. Appl. Mech. Tech. Physics., **42**, 665

[10] Kandasamy, R., Periasamy, K., and Sivagnana Prabhu, K.K., 2005, Effects of chemical reaction, heat and mass transfer along a wedge with heat source and concentration in the presence of suction or injection, Int. J. Heat Mass Transfer, 48, 1388.

[11] Lai, E.c. and Kulacki, F.A., 1990, Effects of variable viscosity on convective heat transfer along a vertical surface in a saturated porous medium, Int. J. Heat Mass Transfer, **33**, 1028.

[12] S. L. Goren, 1977, Thermophoresis of aerosol particles in laminar boundary layer on flat plate, J. Colloid Interface Sci. **61**, 77-85.

[13] Yih, K.A., 1998, Blowing/suction effect on non-Darcy forced convection flow about a flat plate with variable wall temperature in porous media, Acta Mechanica, **131,** 255.

[14] Chamkha, Ali J., 1996, Non-Darcy hydromagnetic free convection from a cone and a wedge in porous media, Int. Comms. Heat Mass Transfer, **23**, 875.

[15] Jayanthi, S and Kumari, M., 2007, Effect of variable viscosity on non-Darcy free or mixed convection flow on a vertical surface in a non-Newtonian fluid saturated porous medium, Appl. Math. Comput., **186**, 1643.

[16] Ching-Yang Cheng, 2006, Non-Darcy natural convection heat and mass transfer from a vertical wavy surface in saturated porous media, Appl. Math. Comput., **182**, 1488.

[17] AI-Odat, M.Q., AI-Hussien, F.M.S and Damesh, R.A., 2005, Influence of radiation on mixed convection over a wedge in non-Darcy porous medium, Forschung im Ingenieurwesen, **69**, 209.

[18] Ali, M. E., 2006, Effect of variable viscosity on mixed convection heat transfer along a vertical moving surface, Int. J. Thermal Sci., **45,** 60.

[19] Elbarbary, E.M.E., Elgazery, N. S., 2004,Chebyshev finite difference method for the effects of variable viscosity and variable thermal conductivity on heat transfer from moving surfaces with radiation, Int. J. Thermal Sci., **43**, 889.

[20] Bejan, A., 1995, Convection heat transfer, p.520, New York: Wiley-Inter Science.

[21] Gill, S., 1951, Proceeding of Cambridge Philosophical Society, pp.96-123.

[22] Minkowycz, W. J., Sparrow, E. M., Schneider, G.E and Pletcher, R.H., Handbook of numerical heat transfer, John Wiley and sons, New York, 1988, pp.192 – 195.

[23] Kafoussias, N.G., and Karabis, A.G., 1996, In proceedings of the 2^{nd} National Congress on Computational Mechanics, Chania, Greece, June 26-28, 1996, vol. II. Edited by D.A. Sotiropoulos and D.E. Beskos., Greek Association of Computational Mechanics, Member of IACM, 801 – 809.

[24] Kafoussias, N.G. and Williams, E.W., 1993, An improved approximation technique to obtain numerical solution of a class of two-point boundary value similarity problems in fluid mechanics, Int. J. Num. Methods Fluids, **17**, 145.

[25] Landau, L.D. and Lifshitz, E.M., Fluid Mechanics, Second Edition, Pergaman Press, lnc., New York, 1962.

Submitted on November 2009, revised on September 2010

Uticaji termoforeze na na nedarsijevski mhd mešoviti konvektivni prenos toplote i mase preko poroznog klina u prisustvu usisavanja i ubrizgavanja

Istražen je uticaj termoforeze taloenja čestica i promenljive viskoznosti na nedarsijevski mešoviti konvektivni prenos toplote i mase od viskoznog nestišljivog i elektroprovodnog fluida preko poroznog klina u prisutnosti usisavanje i ubrizgavanja. Zid klina je ugradjen u uniformni nedarsijevsku poroznu sredinu kako bi se dozvolilo moguće usisavanje ili ubrizgavanje fluida. Parcijalne diferencijalne jednačine problema, podvrgnuti graničnim uslovima, su rešene numerički primenom efikasne šeme rešavanja za lokalnu analizu nesličnosti graničnog sloja. Numerički proračuni su izvedeni za različite vrednosti bezdimenzijskog parametra. Analiza dobijenih pokazuje da na polje tečenja značajno utiče primenjeno magnetsko polje. Rezultati su uporedjeni s onima poznatim iz literature pa se dobija odlično slaganje rezultata.

doi:10.2298/TAM1003203L Math.Subj.Class.: 76W05, 76S05